Synaptopodin regulates denervation-induced homeostatic synaptic plasticity

Andreas Vlachos[a,1], Benno Ikenberg[a], Maximilian Lenz[a], Denise Becker[a], Kurt Reifenberg[b,2], Carlos Bas-Orth[a,3], and Thomas Deller[a]

[a]Institute of Clinical Neuroanatomy, Neuroscience Center, Goethe University Frankfurt, 60590 Frankfurt, Germany; and [b]Central Laboratory Animal Facility, Johannes Gutenberg University, 55131 Mainz, Germany

Edited by Eve Marder, Brandeis University, Waltham, MA, and approved April 4, 2013 (received for review August 8, 2012)

Synaptopodin (SP) is a marker and essential component of the spine apparatus (SA), an enigmatic cellular organelle composed of stacked smooth endoplasmic reticulum that has been linked to synaptic plasticity. However, SP/SA-mediated synaptic plasticity remains incompletely understood. To study the role of SP/SA in homeostatic synaptic plasticity we here used denervation-induced synaptic scaling of mouse dentate granule cells as a model system. This form of plasticity is of considerable interest in the context of neurological diseases that are associated with the loss of neurons and subsequent denervation of connected brain regions. In entorhino-hippocampal slice cultures prepared from SP-deficient mice, which lack the SA, a compensatory increase in excitatory synaptic strength was not observed following partial deafferentation. In line with this finding, prolonged blockade of sodium channels with tetrodotoxin induced homeostatic synaptic scaling in wild-type, but not SP-deficient, slice cultures. By crossing SP-deficient mice with a newly generated transgenic mouse strain that expresses GFP-tagged SP under the control of the Thy1.2 promoter, the ability of dentate granule cells to form the SA and to homeostatically strengthen excitatory synapses was rescued. Interestingly, homeostatic synaptic strengthening was accompanied by a compensatory increase in SP cluster size/stability and SA stack number, suggesting that activity-dependent SP/SA remodeling could be part of a negative feedback mechanism that aims at adjusting the strength of excitatory synapses to persisting changes in network activity. Thus, our results disclose an important role for SP/SA in homeostatic synaptic plasticity.

entorhinal cortex lesion | intracellular calcium stores | NMDA receptors | voltage-gated calcium channels | ryanodine receptors

Homeostatic synaptic scaling is a cellular mechanism that has been described in neuronal networks in which network activity has been perturbed (1–6). It aims at keeping the activity of neurons within a dynamic range and is considered fundamental for physiological network functioning (1–6). Although the specific mechanisms involved in the induction of synaptic scaling depend on the particular conditions of activity perturbation, synaptic scaling requires changes in AMPA receptor (AMPA-R) numbers at excitatory postsynapses (7, 8). It has been suggested that calcium-dependent negative feedback mechanisms control these changes (1–5) and that local protein synthesis of AMPA-R subunits could be involved under certain experimental conditions in "scaling up" excitatory synapses in response to a persisting reduction in neuronal activity (9). Interestingly, several recent reports have shown that homeostatic synaptic plasticity can occur locally, involving some but not all synapses of a neuron (9–14). Thus, local sensors and/or effectors must exist that adjust synaptic strength at individual synapses in a homeostatic manner.

Synaptopodin (SP), an actin-binding protein (15) found in a subset of dendritic spines (16), is an interesting candidate molecule in this context (17–20). SP is a marker and essential component of the spine apparatus (SA) (21, 22), an enigmatic cellular organelle composed of stacked endoplasmic reticulum (22–24) that has been suggested to play a role in the regulation of intracellular calcium levels (25) as well as local protein synthesis (26). SP-deficient animals do not form SAs and show deficits in synaptic plasticity and spatial learning (21, 27). Recently, experimental evidence has been provided that SP clusters colocalize with a functional intracellular source of calcium (28, 29), which, in turn, controls the accumulation of AMPA-R at spine synapses (28, 30). Thus, SP/SA could be one of the sensors and/or effectors of homeostatic synaptic plasticity.

Using entorhinal denervation of organotypic hippocampal slice cultures, we were recently able to demonstrate that deafferented neurons respond to the loss of input with a compensatory (i.e., homeostatic) increase in excitatory synaptic strength (31). This observation is of relevance for neurological diseases associated with neuronal loss and the denervation of connected brain regions. However, although the molecular mechanisms of pharmacologically induced homeostatic synaptic plasticity have been identified to a certain degree (1–6), nothing is currently known about the molecular players involved in denervation-induced synaptic scaling. Here, we provide experimental evidence for an important role of SP/SA in homeostatic synaptic plasticity of denervated neurons.

Results

Organotypic slice cultures containing the entorhinal cortex (EC) and the hippocampus were prepared at postnatal day 4–5 and allowed to mature for 18–21 d in vitro. In these cultures the entorhino-hippocampal projection develops normally (31–33) and can be readily transected, by cutting away the EC from the hippocampus with a scalpel (blue line in Fig. 1*A*). This leads to a partial and lamina-specific denervation of dentate granule cells in the outer molecular layer (OML) without directly damaging the dendritic tree of the targeted neurons (34). Denervated granule cells respond with a homeostatic increase in excitatory synaptic strength (31).

Denervation-Induced Homeostatic Synaptic Strengthening Is Not Observed in SP-Deficient Dentate Granule Cells. Slice cultures prepared from SP-deficient mice were used to study the role of SP/SA in denervation-induced synaptic strengthening. First, the innervation of the dentate gyrus by EC fibers was evaluated using anterograde tracing of the entorhino-hippocampal projection (Fig. 1*B*). Furthermore, we verified that EC fibers form functional excitatory synapses, by stimulating the EC electrically while recording evoked excitatory postsynaptic currents (EPSCs) from dentate granule cells (Fig. 1*C*). On the basis of these observations,

Author contributions: A.V. and T.D. designed research; A.V., B.I., M.L., and D.B. performed research; K.R. and C.B.-O. contributed new reagents/analytic tools; A.V., B.I., M.L., and D.B. analyzed data; and A.V., B.I., M.L., and T.D. wrote the paper.

The authors declare no conflict of interest.

This article is a PNAS Direct Submission.

Freely available online through the PNAS open access option.

[1]To whom correspondence should be addressed. E-mail: a.vlachos@med.uni-frankfurt.de.

[2]Present address: Deutsches Krebsforschungszentrum, 69120 Heidelberg, Germany.

[3]Present address: Department of Neurobiology, Interdisciplinary Center for Neurosciences, University of Heidelberg, 69120 Heidelberg, Germany.

This article contains supporting information online at www.pnas.org/lookup/suppl/doi:10.1073/pnas.1213677110/-/DCSupplemental.

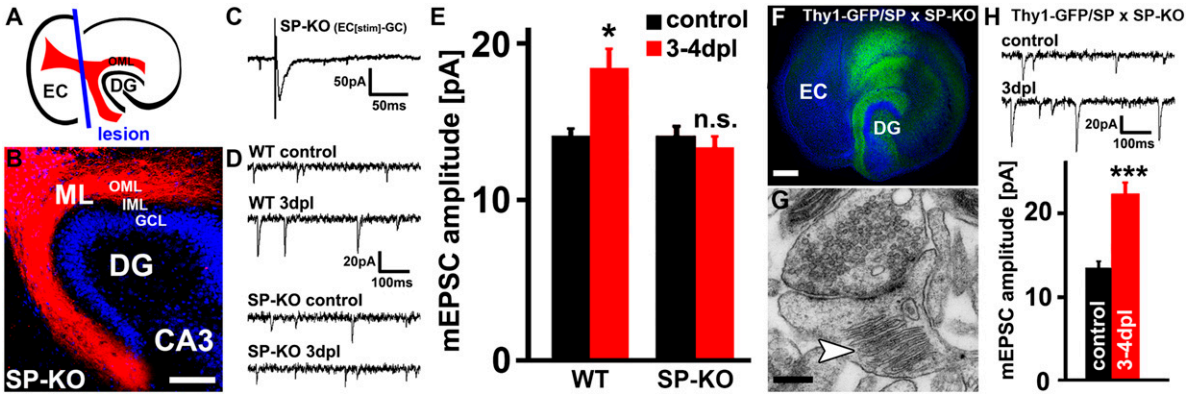

Fig. 1. Denervation-induced homeostatic synaptic strengthening is not observed in SP-deficient dentate granule cells and can be rescued by transgenic expression of GFP/SP. (*A*) Schematic of an entorhino-hippocampal slice culture. The entorhino-hippocampal fiber tract (red) originating from the entorhinal cortex (EC) and terminating in the outer molecular layer (OML) of the dentate gyrus (DG) is illustrated (plane of transection, blue line). (*B*) DiI tracing of entorhino-hippocampal fibers (red; TO-PRO Iodide nuclear stain, blue) revealed the intact entorhino-hippocampal projection in slice cultures prepared from SP-deficient mice (SP-KO). (CA3, cornu ammonis region 3; GCL, granule cell layer; IML, inner molecular layer; ML, molecular layer). (Scale bar: 100 μm.) (*C*) Electrical stimulations of the EC while recording evoked EPSCs from dentate granule cells revealed a functional entorhino-hippocampal projection in SP-deficient cultures. (*D*) Sample traces of miniature excitatory postsynaptic currents (mEPSC) recorded from control, (i.e., nondenervated) and denervated granule cells in wild-type (WT) and SP-deficient cultures. (*E*) A significant increase in the mEPSC amplitude at 3–4 d postlesion (dpl) is observed in WT but not SP-deficient granule cells after denervation (n = 10–14 neurons per group, from four cultures each). (*F*) In slice cultures prepared from Thy1-GFP/SP mice crossed to SP-deficient mice (SP-KO) GFP/SP (green) is regularly seen in the DG. TO-PRO Iodide nuclear stain (blue). (Scale bar: 200 μm.) (*G* and *H*) Expression of GFP/SP rescues the ability of neurons to form spine apparatus organelles (arrowhead) and to express homeostatic synaptic strengthening following denervation (n = 11 neurons per group, from four nondenervated and five denervated cultures). (Scale bar in *G*: 0.2 μm.) *P < 0.05; ***P < 0.001; NS, not significant.

we concluded that a functional entorhino-hippocampal projection is present in SP-deficient cultures.

Subsequently, entorhinal denervation was performed and changes in excitatory synaptic strength were assessed at 3–4 d postlesion (dpl) by recording miniature EPSCs (mEPSCs) from dentate granule cells of wild-type and SP-deficient cultures (Fig. 1*D*). At this time point the denervation-induced increase in synaptic strength has reached a plateau (31). Although no significant differences in mean mEPSC frequencies were observed between the groups (wild-type, control 2.3 ± 0.2 Hz and 3–4 dpl 2.9 ± 0.4 Hz, $P = 0.21$; SP-deficient, control 2.3 ± 0.2 Hz and 3–4 dpl 3.0 ± 0.3 Hz, $P = 0.11$; no difference between wild-type and SP-deficient cultures), a significant increase in mEPSC amplitudes was only observed in denervated wild-type cultures and not in SP-deficient granule cells (Fig. 1*E*). This finding suggested a role for SP/SA in denervation-induced homeostatic synaptic plasticity.

Tetrodotoxin-Induced Homeostatic Synaptic Strengthening Is Impaired in SP-Deficient Dentate Granule Cells. To confirm these results and to exclude that the inability of SP-deficient granule cells to express synaptic scaling following entorhinal denervation is the result of subtle alterations in innervation, which may have escaped our detection, a classical pharmacological approach, tetrodotoxin (TTX) treatment (13, 14, 35–37), was used to induce synaptic scaling. In contrast to TTX-treated (2 μM; 2–3 d) wild-type dentate granule cells, prolonged TTX treatment of SP-deficient granule cells failed to significantly increase mEPSC amplitudes (Fig. S1 *A* and *B*). Together, these results demonstrated an important role for SP/SA in homeostatic synaptic plasticity of dentate granule cells in vitro, both under conditions of partial denervation and pharmacological blockade of neuronal activity.

Expression of GFP/SP Rescues the Ability of SP-Deficient Dentate Granule Cells to Form SAs and to Homeostatically Increase Excitatory Synaptic Strength. To corroborate the above findings and to follow the dynamics of SP in individual living neurons, a transgenic mouse strain, which expresses GFP-tagged SP under the control of the Thy1.2 promoter, was generated (Fig. S2). By crossing this strain with SP-deficient animals we obtained mice that lack endogenous SP and only express GFP/SP (Thy1-GFP/SP × SP-KO mice; details are given in *SI Materials and Methods*). In cultures prepared from these mice GFP/SP expression was regularly seen in the dentate gyrus (Fig. 1*F*). Of note, the ability of SP-deficient granule cells to form SAs was rescued in these cultures by the expression of GFP/SP (Fig. 1*G*).

After confirming the presence of a functional entorhino-hippocampal projection, we applied the two protocols (denervation, Fig. 1*H*; TTX, Fig. S1*C*) to test for homeostatic synaptic strengthening in slice cultures of Thy1-GFP/SP × SP-KO mice. Indeed, expression of GFP/SP was sufficient to rescue the ability of SP-deficient granule cells to increase their excitatory strength under both conditions.

Early Phase of Denervation-Induced Synaptic Scaling Requires the Presence of SP/SA. Because it has been indicated that synaptic scaling may be divided into molecularly distinct phases (38), the role of SP was also assessed during the earlier phase of denervation-induced synaptic scaling. At 1 dpl no significant increase in mEPSC amplitudes was detected in SP-deficient granule cells, whereas transgenic expression of GFP/SP rescued the scaling response of denervated dentate granule cells (Fig. S3), similar to what was observed at 3–4 dpl. Taken together, we concluded that the ability of cultured dentate granule cells to express homeostatic synaptic plasticity depends on the presence of SP and the SA organelle.

Denervation-Induced Homeostatic Synaptic Plasticity Is Accompanied by an Enlargement of SP Clusters. To provide further experimental evidence that SP is linked to denervation-induced homeostatic plasticity, we next addressed the question of whether homeostatic synaptic strengthening is accompanied by compensatory structural changes of SP/SA. In this set of experiments we exploited the fact that entorhinal denervation leads to a layer-specific increase in synaptic strength at 3–4 dpl, that is, to homeostatic strengthening of excitatory synapses predominantly in the OML (31). Denervated (3–4 dpl) and age-matched nondenervated wild-type cultures were fixed and stained for endogenous SP (Fig. 2*A*; specificity of antibody tested in tissue from SP-deficient mice, Fig. S2*F*) and the sizes of immunofluorescent endogenous SP clusters were assessed in the

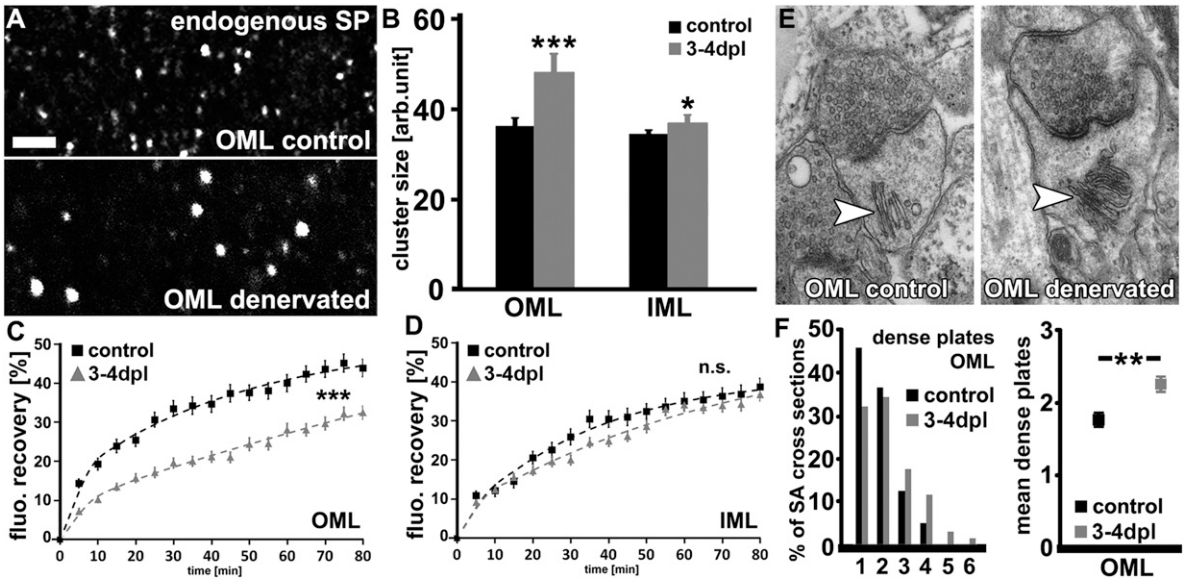

Fig. 2. Denervation-induced homeostatic synaptic scaling is accompanied by structural changes of SP clusters and SA organelles. (*A*) Control and denervated wild-type cultures were stained for endogenous SP and mean cluster sizes were determined in the OML and IML. (Scale bar: 2 μm.) (*B*) A considerable increase in mean SP cluster sizes was detected in the OML following denervation. In the IML the effect was less pronounced (n = 6–10 cultures per group, three visual fields per culture). (*C*) Quantitative evaluation of GFP/Sp cluster fluorescent recovery after photobleaching (FRAP). Statistical comparisons performed with averaged values between 65–80 min per cluster (details given in *SI Materials and Methods*; n = 86 clusters from 12 control cultures; n = 70 clusters from 9 denervated cultures; six to nine clusters bleached per culture). (*D*) No significant difference in FRAP of GFP/SP clusters was observed in the IML of control and denervated cultures. (n = 54 clusters from eight control cultures; n = 52 clusters from seven denervated cultures; six to nine clusters bleached per culture). (*E* and *F*) The mean stack number of SAs was increased in the OML after denervation (n = 120–137 SAs in six cultures each; 20–25 SAs per culture). $^{**}P < 0.01$; $^{***}P < 0.001$; NS, not significant.

denervated OML and the nondenervated inner molecular layer (IML) (39–41). The results of these experiments disclosed a significant increase in SP cluster size of ∼35% in the denervated OML in comparison with nondenervated control cultures, whereas in the IML only a small (∼5%) increase in SP cluster sizes was observed (Fig. 2*B*). We concluded that denervation-induced homeostatic synaptic plasticity is accompanied by an increase in SP cluster sizes.

Denervation-Induced Homeostatic Synaptic Plasticity Is Accompanied by an Increase in SP Cluster Stability. In an attempt to evaluate whether the dynamics of SP clusters were affected by deafferentation, fluorescence recovery after photobleaching (FRAP) of GFP/SP clusters was determined in the OML and IML of control and denervated cultures (3–4 dpl, Fig. 2 *C* and *D*). Following a 15-min baseline recording (ΔT = 5 min), individual GFP/SP clusters were bleached (<5% of initial fluorescence). The reappearance of GFP fluorescence was then followed for up to 80 min at 5-min intervals. The results revealed a highly significant difference in the FRAP of GFP/SP clusters in the OML. In control cultures, a comparatively fast recovery was observed such that 30% of the averaged prebleach GFP/SP fluorescence recovered within 20–30 min after photobleaching (Fig. 2*C*). In contrast, following the induction of homeostatic synaptic plasticity 30% recovery was reached ∼80 min after the bleach (biexponential fitting of FRAP curves is given in *SI Materials and Methods*). Notably, the difference in FRAP of GFP/SP clusters in control and denervated cultures was still seen when clusters of equal size were compared (Fig. S4*A*), suggesting that SP cluster size does not determine GFP/SP cluster FRAP. Taken together, these data showed that the turnover of GFP/SP clusters is slowed following entorhinal denervation. Because partial deafferentation did not change the FRAP of GFP/SP clusters in the nondenervated IML (Fig. 2*D*), we concluded that SP cluster stability is mainly affected in the layer of denervation (i.e., the layer in which synaptic strength is scaled up at 3–4 dpl) (13).

To further strengthen these findings, SP cluster properties were evaluated in the OML during the early phase after denervation (between 0 and 6 h, 6 and 12 h, and 12 and 24 h following deafferentation) (Fig. S4 *B–D*). Indeed, a close interrelation between SP cluster remodeling, that is, an increase in SP cluster size/stability, and the induction of synaptic scaling was evident in these experiments. Of note, SP-mRNA levels were not significantly increased at 1, 2, and 4 dpl in the granule cell layer as determined by laser capture microdissection (LMD)-quantitative PCR analysis (Fig. S5), indicating that the observed changes are not regulated via changes of mRNA levels as seen following the induction of long-term potentiation (LTP) (42, 43). In summary, the results of these experiments disclosed that denervation-induced homeostatic synaptic strengthening is accompanied by an increase in SP cluster size and stability.

Denervation-Induced Ultrastructural Changes of SA Organelles. The SP cluster analysis led us to the hypothesis that ultrastructural hallmarks of the SA could change after denervation. Because SP seems to be enriched in the so-called dense plates (22), which are localized between the stacked cisternae of smooth endoplasmic reticulum (22–24), we reasoned that changes in SP immunohistochemistry and FRAP, that is, reduced turnover and increased size of SP clusters after denervation, might reflect changes in the number of SA stacks, (i.e., changes in mean dense plate number). Hence, we subjected control and denervated cultures to EM analysis and cross-sections of SAs were assessed in the OML and IML. Whereas in control cultures 46% of identified SA cross-sections revealed single dense plates (i.e., two endoplasmic cisternae) and only 5% contained four or more dense plates, in the OML of denervated cultures 32% of SA cross-sections disclosed single dense plates and now 16% demonstrated four or more dense plates (Fig. 2 *E* and *F*). In line with this shift toward higher stack numbers of the SA, our analysis also revealed a significant increase in the mean stack number of SAs in the OML of denervated cultures (Fig. 2*F*). In the IML a slight increase in mean dense plate number was also seen

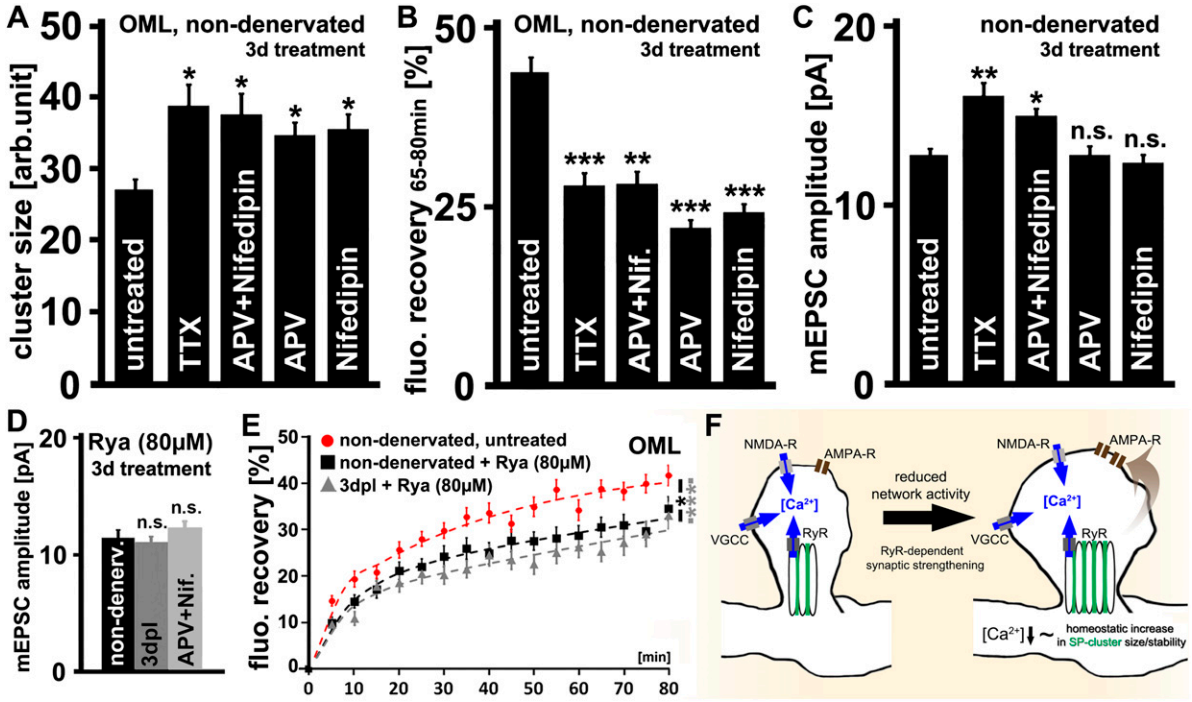

Fig. 3. The role of neuronal activity and ryanodine receptors (RyRs) in SP cluster remodeling and denervation-induced homeostatic synaptic strengthening. (*A* and *B*) In nondenervated wild-type cultures treatment with TTX (2 μM), APV (50 μM) + Nifedipin (20 μM), and APV or Nifedipin alone for 3 d resulted an increase in (*A*) Sp cluster sizes (n = 5–13 cultures per group; three to six visual fields per cultures) and (*B*) GFP/Sp cluster FRAP (n = 24–86 clusters per group; three to four cultures per group; statistical comparison performed with mean FRAP values between 65–80 min after bleaching). (*C*) Whereas TTX and APV+ Nifedipin treatment increased mEPSC amplitudes as seen following denervation, APV or Nifedipin alone had no significant effect on mean mEPSC amplitude (n = 11–21 neurons per group; from four to eight cultures, each). (*D*) Inhibition of RyRs with a high dose of ryanodine (80 μM, 3 d) impairs denervation- and APV+Nifedipin-induced homeostatic synaptic strengthening (n = 13–15 neurons from four to six cultures each). (*E*) In the presence of ryanodine (80 μM) a reduction in GFP/SP cluster FRAP was observed in both nondenervated and denervated cultures (n = 34–38 clusters from five cultures each; six to nine clusters bleached per culture). The effects of ryanodine treatment and denervation were not additive. (*F*) Model of SP-dependent homeostatic synaptic plasticity. A reduction in neuronal activity leads to a compensatory increase in SP cluster sizes and SA stacking. SP remodeling may be part of a calcium-dependent negative feedback mechanism that promotes the ability of synapses to efficiently accumulate AMPA-R at excitatory synapses via a not-yet-fully-understood SP/SA-dependent mechanism. Earlier work has linked SP to spines with a bigger spine head volume and revealed that SP clusters associate with an intracellular source of calcium (28, 29) which regulates the accumulation of AMPA-R at excitatory postsynapses in a RyR-dependent manner (28). *P < 0.05; **P < 0.01; ***P < 0.001; NS, not significant.

(control IML, 2.60 ± 0.11 vs. 3–4 dpl, 3.0 ± 0.14; P = 0.033). These results reflected, at least in part, our immunohistochemistry and FRAP data (Fig. 2 *A–D*) and showed that SAs can change their stack number in response to denervation. We concluded that a compensatory increase in SA stacking accompanies the induction of denervation-induced homeostatic synaptic plasticity.

SP/SA Remodeling Is Regulated Inversely by Neuronal Activity. The above findings raised the possibility that SP/SA remodeling could be part of an activity-dependent negative-feedback mechanism that aims at adjusting synaptic strength in a homeostatic manner (1, 3). Based on this theory we hypothesized that a reduction in neuronal activity, reflected by a decrease in intracellular [Ca^{2+}], could induce the compensatory increase in SP cluster sizes and stability, which could in turn promote the accumulation of AMPA-R at excitatory postsynapses (28).

To learn more about the mechanisms that control SP cluster properties in the context of homeostatic synaptic scaling, pharmacological inhibition of network activity of nondenervated cultures with TTX (2 μM, 3 d) was used first. Indeed, the effects of entorhinal denervation on SP cluster sizes (Fig. 3*A*), GFP/SP cluster FRAP (Fig. 3*B*), and SA stacking (Fig. S6), as well as changes in mEPSC amplitudes (Fig. 3*C*), were mimicked by the TTX treatment. To test for the role of Ca^{2+} entry sites in this context, nondenervated cultures were treated for 3 d with the NMDA receptor (NMDA-R) inhibitor R-2-amino-5-phosphonopentanoate (APV, 50 μM) and Nifedipin (20 μM), which blocks L-type voltage-gated calcium channels (L-VGCC). Indeed, combined APV+Nifedipin treatment revealed results comparable to those seen following TTX treatment and denervation (Fig. 3 *A–C*).

We then determined whether inhibition of NMDA-R or L-VGCC underlies the observed changes. Interestingly, APV or Nifedipin treatment increased SP cluster size and stability while leaving mEPSC amplitudes unchanged (Fig. 3 *A–C*). Taken together, these results suggested that a reduction in neuronal activity (i.e., intracellular calcium levels) could trigger a compensatory increase in SP cluster size and stability. However, these changes seem to be insufficient to induce homeostatic synaptic scaling. Only when both NMDA-R and L-VGCC are blocked for 3 d is an increase in excitatory synaptic strength induced in cultured dentate granule cells.

Denervation-Induced Homeostatic Synaptic Strengthening Depends on Ryanodine Receptor Activity. Previous work has revealed that SP clusters associate with ryanodine receptors (RyRs), which in turn promote the accumulation of AMPA-R at excitatory postsynapses of SP-containing dendritic spines (28). We therefore tested whether RyRs could also be involved in denervation-induced homeostatic synaptic strengthening. Nondenervated control cultures and denervated cultures were treated for 3 d with a high dose of ryanodine (80 μM) to block RyRs (44, 45) and mEPSCs were subsequently recorded. In the case of denervation RyRs were blocked immediately after lesioning. Because a compensatory

increase in excitatory synaptic strength was not observed under these conditions (Fig. 3*D*), our results suggested that RyR activity is required for the homeostatic synaptic strengthening response of cultured dentate granule cells at 3–4 dpl. Ryanodine treatment also inhibited the APV+Nifedipin-induced increase in mEPSC amplitudes of nondenervated dentate granule cells (Fig. 3*D*).

Finally, we tested for the effects of RyR blockade on SP cluster properties. Control and denervated cultures were treated with ryanodine and SP cluster sizes and GFP/SP cluster FRAP were assessed in the OML. In these experiments an increase in SP cluster size (untreated, 26.9 ± 1.5; ryanodine, 36.1 ± 1.4; $P < 0.05$) and stability (Fig. 3*E*) was observed in nondenervated cultures. Because denervation and RyR blockade were not additive in their effects on GFP/SP cluster FRAP (Fig. 3*E*), we concluded that similar mechanisms (i.e., a reduction in RyR activity) may account, at least in part, for the denervation-induced stabilization of SP clusters.

Discussion

The major finding of our study is based on the observation that neither entorhinal denervation nor TTX treatment induced homeostatic strengthening of excitatory synapses in SP-deficient dentate granule cells. We could rescue the ability of SP-deficient neurons to form SAs and to express denervation- as well as TTX-dependent homeostatic synaptic plasticity with transgenic expression of GFP/SP. This finding is in line with previous work that showed that SP is part of the receptor trafficking machinery that regulates the accumulation of AMPA-R at excitatory postsynapses and, thus, excitatory synaptic strength (28, 30). Our data now disclose an important role for SP in homeostatic synaptic plasticity of dentate granule cells in vitro.

The ability of neurons to adjust their synaptic strength in a homeostatic manner is considered to depend on negative feedback mechanisms that sense the activity of a neuron and regulate receptor trafficking to increase or decrease synaptic strength (1–5). It has been suggested that calcium-dependent negative feedback mechanisms play an important role in this context (1–5). However, the sensors and effectors of homeostatic synaptic plasticity remain insufficiently understood, specifically in the context of local homeostatic synaptic plasticity (5). Using entorhinal denervation and pharmacological treatment of nondenervated cultures, we now demonstrate that the loss of input and a prolonged reduction in neuronal activity lead to a compensatory increase in SP cluster sizes and stability as well as SA stacking. The effects of denervation and TTX treatment on SP clusters were mimicked by pharmacological inhibition of NMDA-R, L-VGCC, or RyR. These data indicate that SP/SA remodeling could be part of the proposed calcium-dependent negative feedback mechanism that aims at readjusting excitatory synaptic strength in response to a persisting reduction in neuronal network activity (Fig. 3*F*).

Interestingly, inhibition of NMDA-R or L-VGCC alone induced an increase in SP cluster size and stability without affecting mEPSC amplitudes. In contrast, blockade of both NMDA-R and L-VGCC for 3 d caused an increase in SP cluster size and mEPSC amplitudes. This finding raises the intriguing possibility that SP/SA may be part of a coincidence-detection machinery involved in the local regulation of excitatory synaptic strength. In line with this concept a local reduction in synaptic activity could cause an increase in SP/SA sizes without affecting synaptic strength. Likewise, a prolonged reduction in neuronal activity, that is, neuronal firing and/or dendritic spiking, may alter SP/SA properties but not synaptic strength. Only if both local synaptic and global neuronal activity are reduced is the molecular machinery that leads to the SP-dependent homeostatic increase in excitatory synaptic strength functional. Notably, experimental evidence has been provided that the combined inhibition of network activity and local NMDA-R inhibition leads to the activation of local protein synthesis (9). Because SAs have also been implicated in local protein synthesis (26), it is interesting to speculate that SP/SA remodeling is a first step that prepares synapses for later changes, such as an accumulation of AMPA-R at postsynaptic sites, for instance via local mRNA translation and/or trafficking of AMPA-R subunits.

In earlier work we were able to demonstrate that SP clusters colocalize with a functional RyR-containing intracellular source of calcium, which in turn controls the accumulation of AMPA-R at excitatory postsynapses of SP-containing spines (28). Our current data support this finding, because denervation- and APV+Nifedipin-induced homeostatic synaptic strengthening were impaired when RyRs were pharmacologically blocked. Although it will now be important to identify the up- and downstream mechanisms of SP/SA-dependent RyR-mediated homeostatic synaptic plasticity (see ref. 46), the results concur, at least in part, with a recent study in which TTX-induced homeostatic changes at CA3 mossy-fiber synapses were blocked by pharmacological depletion of intracellular calcium stores with thapsigargin (14). Interestingly, SP/SA is regularly found at this synapse (22, 39, 47). Thus, SP/SA may assert its effects on homeostatic synaptic plasticity as an intracellular source of calcium. Apparently, the precise mechanisms through which SP/SA regulate synaptic strength warrant further investigation (Fig. 3*F*).

Previous work has linked SP/SA to Hebbian forms of synaptic plasticity (21, 27, 28). Although under certain experimental conditions an interdependence between SP expression levels and the ability to induce LTP was not found (40), it has also been shown that a transient activation of NMDA-R can cause an accumulation of SP in spines (28), which is consistent with a report demonstrating increased SP levels upon electrical induction of LTP in vivo (48). Although seemingly contradictory to the findings of the present study, these results are well in line with the view that distinct molecular mechanisms control homeostatic and Hebbian forms of synaptic plasticity (3). According to this concept, different signaling pathways could target SP/SA (and its structural remodeling) as an essential component of the downstream effector machinery regulating AMPA-R accumulation at spine synapses. Thus, an increase in SP cluster sizes (and SA stacking) could serve the efficient accumulation of AMPA-Rs at excitatory postsynapses under both Hebbian and homeostatic conditions (20). It will now be interesting to test for the effects of other signaling pathways known to regulate Hebbian or homeostatic synaptic plasticity on SP/SA remodeling. Moreover, new, important insights into the role of SP/SA in synaptic plasticity under physiological and pathological conditions may be acquired by testing whether the suggested SA/SP-dependent "homeostatic sensitization" of excitatory synapses, reflected by the increase in SP/SA size following APV, Nifedipin, or ryanodine treatment, could affect the ability of synapses to express synaptic plasticity (i.e., to show metaplasticity) (49).

Materials and Methods

Animals. The following mouse strains were used in the present study: wild-type C57BL/6 mice, SP-deficient mice [internal strain designation SP-KO; official strain designation C57BL/6-Synpo^{tm1Mif} (21)], and a newly generated transgenic mouse line expressing GFP-tagged SP under the control of the Thy1.2 promoter crossed to SP-deficient mice (Thy1-GFP/SP × SP-KO).

Generation of Thy1-GFP/SP Transgenic Mice. Details are given in *SI Materials and Methods*.

Preparation of Slice Cultures. Entorhino-hippocampal slice cultures were prepared as described previously (31, 33).

Whole-Cell Patch-Clamp Recordings. Whole-cell voltage recordings were carried out as described in ref. 31.

Fluorescent Recovery After Photobleaching Analysis. FRAP experiments were performed and analyzed as previously described (50). Information is also given in *SI Materials and Methods*.

Immunostaining. Cultures were fixed and stained as previously described (34) with antibodies against synaptopodin (SE-19; Sigma; 1:1,000).

Electron Microscopy. Details are provided in *SI Materials and Methods*.

Laser Capture Microdissection and Quantitative PCR. The granule cell layer of denervated cultures and age-matched nondenervated control cultures was isolated from 10-μm-thick resliced cultures using LMD as previously described (51). The probes were subjected to quantitative PCR analysis. Further details are provided in *SI Materials and Methods*.

Quantification and Statistics. Electrophysiological data were analyzed as described in ref. 31. The Image-J software package (http://rsb.info.nih.gov/ij) was used to analyze immunostainings and FRAP (50); details are provided in *SI Materials and Methods*. Immunostainings were analyzed as described before (e.g., ref. 39). For EM, identified cross-sections of SAs were assessed in the respective regions and the number of dense plates and endoplasmic cisternae was noted. SA stacks were defined as x dense plates and $x + 1$ cisternae. Data obtained by quantitative PCR were analyzed as described by Pfaffl (52). Statistical comparisons were made using the Wilcoxon–Mann–Whitney test or Kruskal–Wallis test followed by Dunn's post hoc analysis to correct for multiple comparisons. P values of less than 0.05 were considered a significant difference. All values represent means ± SEM.

ACKNOWLEDGMENTS. We thank Charlotte Nolte-Uhl, Nadine Zahn, and Anke Biczysko for excellent technical assistance; Dr. P. Mundel for providing the GFP/SP plasmid; and Dr. P. Caroni for providing the Thy1.2-promoter. The work was supported by Josef-Buchmann-Stipendienfonds (B.I.), a Young Investigators Grant and the Junior Researchers in Focus Program of Goethe University (to A.V.), German–Israeli Foundation Grants GIF G-2239-2096.1/2009 (to A.V.) and GIF 827/04 (to T.D.), and by Deutsche Forschungsgemeinschaft Grants DFG DE 551/10-1 (to T.D.) and CRC 1080 (to A.V. and T.D.).

1. Davis GW (2006) Homeostatic control of neural activity: From phenomenology to molecular design. *Annu Rev Neurosci* 29:307–323.
2. Marder E, Goaillard JM (2006) Variability, compensation and homeostasis in neuron and network function. *Nat Rev Neurosci* 7(7):563–574.
3. Turrigiano GG (2008) The self-tuning neuron: Synaptic scaling of excitatory synapses. *Cell* 135(3):422–435.
4. Pozo K, Goda Y (2010) Unraveling mechanisms of homeostatic synaptic plasticity. *Neuron* 66(3):337–351.
5. Turrigiano G (2012) Homeostatic synaptic plasticity: Local and global mechanisms for stabilizing neuronal function. *Cold Spring Harb Perspect Biol* 4(1):a005736.
6. Vitureira N, Letellier M, Goda Y (2012) Homeostatic synaptic plasticity: From single synapses to neural circuits. *Curr Opin Neurobiol* 22(3):516–521.
7. Turrigiano GG, Leslie KR, Desai NS, Rutherford LC, Nelson SB (1998) Activity-dependent scaling of quantal amplitude in neocortical neurons. *Nature* 391(6670): 892–896.
8. O'Brien RJ, et al. (1998) Activity-dependent modulation of synaptic AMPA receptor accumulation. *Neuron* 21(5):1067–1078.
9. Sutton MA, et al. (2006) Miniature neurotransmission stabilizes synaptic function via tonic suppression of local dendritic protein synthesis. *Cell* 125(4):785–799.
10. Branco T, Staras K, Darcy KJ, Goda Y (2008) Local dendritic activity sets release probability at hippocampal synapses. *Neuron* 59(3):475–485.
11. Hou Q, Zhang D, Jarzylo L, Huganir RL, Man HY (2008) Homeostatic regulation of AMPA receptor expression at single hippocampal synapses. *Proc Natl Acad Sci USA* 105(2):775–780.
12. Kim J, Tsien RW (2008) Synapse-specific adaptations to inactivity in hippocampal circuits achieve homeostatic gain control while dampening network reverberation. *Neuron* 58(6):925–937.
13. Mitra A, Mitra SS, Tsien RW (2012) Heterogeneous reallocation of presynaptic efficacy in recurrent excitatory circuits adapting to inactivity. *Nat Neurosci* 15(2):250–257.
14. Lee KJ, et al. (2013) Mossy fiber-CA3 synapses mediate homeostatic plasticity in mature hippocampal neurons. *Neuron* 77(1):99–114.
15. Mundel P, et al. (1997) Synaptopodin: An actin-associated protein in telencephalic dendrites and renal podocytes. *J Cell Biol* 139(1):193–204.
16. Deller T, Mundel P, Frotscher M (2000) Potential role of synaptopodin in spine motility by coupling actin to the spine apparatus. *Hippocampus* 10(5):569–581.
17. Deller T, et al. (2007) A role for synaptopodin and the spine apparatus in hippocampal synaptic plasticity. *Ann Anat* 189(1):5–16.
18. Jedlicka P, Vlachos A, Schwarzacher SW, Deller T (2008) A role for the spine apparatus in LTP and spatial learning. *Behav Brain Res* 192(1):12–19.
19. Segal M, Vlachos A, Korkotian E (2010) The spine apparatus, synaptopodin, and dendritic spine plasticity. *Neuroscientist* 16(2):125–131.
20. Vlachos A (2012) Synaptopodin and the spine apparatus organelle-regulators of different forms of synaptic plasticity? *Ann Anat* 194(4):317–320.
21. Deller T, et al. (2003) Synaptopodin-deficient mice lack a spine apparatus and show deficits in synaptic plasticity. *Proc Natl Acad Sci USA* 100(18):10494–10499.
22. Deller T, Merten T, Roth SU, Mundel P, Frotscher M (2000) Actin-associated protein synaptopodin in the rat hippocampal formation: Localization in the spine neck and close association with the spine apparatus of principal neurons. *J Comp Neurol* 418(2): 164–181.
23. Gray EG (1959) Axo-somatic and axo-dendritic synapses of the cerebral cortex: An electron microscope study. *J Anat* 93:420–433.
24. Spacek J, Harris KM (1997) Three-dimensional organization of smooth endoplasmic reticulum in hippocampal CA1 dendrites and dendritic spines of the immature and mature rat. *J Neurosci* 17(1):190–203.
25. Fifková E, Markham JA, Delay RJ (1983) Calcium in the spine apparatus of dendritic spines in the dentate molecular layer. *Brain Res* 266(1):163–168.
26. Pierce JP, van Leyen K, McCarthy JB (2000) Translocation machinery for synthesis of integral membrane and secretory proteins in dendritic spines. *Nat Neurosci* 3(4): 311–313.
27. Jedlicka P, et al. (2009) Impairment of in vivo theta-burst long-term potentiation and network excitability in the dentate gyrus of synaptopodin-deficient mice lacking the spine apparatus and the cisternal organelle. *Hippocampus* 19(2):130–140.
28. Vlachos A, et al. (2009) Synaptopodin regulates plasticity of dendritic spines in hippocampal neurons. *J Neurosci* 29(4):1017–1033.
29. Korkotian E, Segal M (2011) Synaptopodin regulates release of calcium from stores in dendritic spines of cultured hippocampal neurons. *J Physiol* 589(Pt 24):5987–5995.
30. Holbro N, Grunditz A, Oertner TG (2009) Differential distribution of endoplasmic reticulum controls metabotropic signaling and plasticity at hippocampal synapses. *Proc Natl Acad Sci USA* 106(35):15055–15060.
31. Vlachos A, et al. (2012) Entorhinal denervation induces homeostatic synaptic scaling of excitatory postsynapses of dentate granule cells in mouse organotypic slice cultures. *PLoS ONE* 7(3):e32883.
32. Frotscher M, Heimrich B (1993) Formation of layer-specific fiber projections to the hippocampus in vitro. *Proc Natl Acad Sci USA* 90(21):10400–10403.
33. Vlachos A, Bas Orth C, Schneider G, Deller T (2012) Time-lapse imaging of granule cells in mouse entorhino-hippocampal slice cultures reveals changes in spine stability after entorhinal denervation. *J Comp Neurol* 520(9):1891–1902.
34. Müller CM, Vlachos A, Deller T (2010) Calcium homeostasis of acutely denervated and lesioned dentate gyrus in organotypic entorhino-hippocampal co-cultures. *Cell Calcium* 47(3):242–252.
35. Ibata K, Sun Q, Turrigiano GG (2008) Rapid synaptic scaling induced by changes in postsynaptic firing. *Neuron* 57(6):819–826.
36. Wierenga CJ, Ibata K, Turrigiano GG (2005) Postsynaptic expression of homeostatic plasticity at neocortical synapses. *J Neurosci* 25(11):2895–2905.
37. Gainey MA, Hurvitz-Wolff JR, Lambo ME, Turrigiano GG (2009) Synaptic scaling requires the GluR2 subunit of the AMPA receptor. *J Neurosci* 29(20):6479–6489.
38. Steinmetz CC, Turrigiano GG (2010) Tumor necrosis factor-α signaling maintains the ability of cortical synapses to express synaptic scaling. *J Neurosci* 30(44):14685–14690.
39. Bas Orth C, et al. (2005) Lamina-specific distribution of Synaptopodin, an actin-associated molecule essential for the spine apparatus, in identified principal cell dendrites of the mouse hippocampus. *J Comp Neurol* 487(3):227–239.
40. Vlachos A, Maggio N, Segal M (2008) Lack of correlation between synaptopodin expression and the ability to induce LTP in the rat dorsal and ventral hippocampus. *Hippocampus* 18(1):1–4.
41. Deller T, et al. (2006) Plasticity of synaptopodin and the spine apparatus organelle in the rat fascia dentata following entorhinal cortex lesion. *J Comp Neurol* 499(3): 471–484.
42. Yamazaki M, Matsuo R, Fukazawa Y, Ozawa F, Inokuchi K (2001) Regulated expression of an actin-associated protein, synaptopodin, during long-term potentiation. *J Neurochem* 79(1):192–199.
43. Okubo-Suzuki R, Okada D, Sekiguchi M, Inokuchi K (2008) Synaptopodin maintains the neural activity-dependent enlargement of dendritic spines in hippocampal neurons. *Mol Cell Neurosci* 38(2):266–276.
44. McPherson PS, et al. (1991) The brain ryanodine receptor: A caffeine-sensitive calcium release channel. *Neuron* 7(1):17–25.
45. Rousseau E, Smith JS, Meissner G (1987) Ryanodine modifies conductance and gating behavior of single Ca2+ release channel. *Am J Physiol* 253(3 Pt 1):C364–C368.
46. Kakizawa S, et al. (2012) Nitric oxide-induced calcium release via ryanodine receptors regulates neuronal function. *EMBO J* 31(2):417–428.
47. Hamlyn LH (1962) The fine structure of the mossy fibre endings in the hippocampus of the rabbit. *J Anat* 96:112–120.
48. Fukazawa Y, et al. (2003) Hippocampal LTP is accompanied by enhanced F-actin content within the dendritic spine that is essential for late LTP maintenance in vivo. *Neuron* 38(3):447–460.
49. Abraham WC (2008) Metaplasticity: Tuning synapses and networks for plasticity. *Nat Rev Neurosci* 9(5):387.
50. Vlachos A, Reddy-Alla S, Papadopoulos T, Deller T, Betz H (2012) Homeostatic regulation of Gephyrin scaffolds and synaptic strength at mature hippocampal GABAergic postsynapses. *Cereb Cortex*, 10.1093/cercor/bhs260.
51. Burbach GJ, Dehn D, Del Turco D, Deller T (2003) Quantification of layer-specific gene expression in the hippocampus: Effective use of laser microdissection in combination with quantitative RT-PCR. *J Neurosci Methods* 131(1-2):83–91.
52. Pfaffl MW (2001) A new mathematical model for relative quantification in real-time RT-PCR. *Nucleic Acids Res* 29(9):e45.